IEEE Access
Multidisciplinary | Rapid Review | Open Access Journal

Received February 19, 2020, accepted March 9, 2020, date of publication April 21, 2020, date of current version May 6, 2020.

Digital Object Identifier 10.1109/ACCESS.2020.2989235

Exploring Uplink Achievable Rate for HPO MIMO Through Quasi-Monte Carlo and Variance Reduction Techniques

YI GONG[1,2], (Student Member, IEEE), LIN ZHANG[1], (Member, IEEE), KEPING YU[3,4], (Member, IEEE), AND RENPING LIU[2], (Senior Member, IEEE)

[1]School of Information and Communication Engineering, Beijing University of Posts and Telecommunications (BUPT), Beijing 100876, China
[2]Global Big Data Technologies Centre (GBDTC), University of Technology Sydney (UTS), Sydney, NSW 2007, Australia
[3]Global Information and Telecommunication Institute, Waseda University, Tokyo 169-8050, Japan
[4]Shenzhen Boyi Technology Company, Ltd., Shenzhen 518125, China

Corresponding author: Lin Zhang (zhanglin@bupt.edu.cn)

This work was supported in part by the Industrial Internet Research Institute (Jinan) of BUPT under Grant 201915001, and in part by the University of Technology Sydney (UTS) in Australia.

ABSTRACT The power consumption at the receiver side will be dramatically increased in the millimetre-wave and massive multiple-input-multiple-output (MIMO) communication systems due to the wide bandwidth and a large number of antennas adopted. A half phase-only MIMO (HPO MIMO) scheme, in which the base station (BS) acquires π-periodic phase measurements of the complex envelop signals was proposed very recently to overcome the above problem. Due to the non-linear nature of HPO MIMO, the valuation of the achievable rate is very challenging. The purpose of the paper is to provide an efficient method for calculating the achievable rate of the HPO MIMO system. By the mutual information theory, we transform the achievable rate into a sum of two high-dimensional integrations. However, calculating those integrations suffers from the enormous computational burden when using the traditional Monte-Carlo method. In order to increase efficiency, a new method by combining quasi-Monte Carlo with a variance reduction technique is proposed. Besides, we derive the probability density function (PDF) of the HPO MIMO system and analyze the uplink achievable rate of the HPO MIMO scheme. Numerical results show that our proposed method is efficient for calculating the achievable rate of the HPO MIMO system. With the proposed method we confirm that HPO MIMO is a promising technology in future low-power communication scenarios.

INDEX TERMS Achievable rate, information capacity, non-linear MIMO, quasi-Monte Carlo, variance reduction.

I. INTRODUCTION

Multiple-input-multiple-output (MIMO) supports multiple data streams simultaneously and enhances data transmission reliability by adopting multiple radio-frequency (RF) chains at both the transmitter and receiver sides. This technology provides technical assurance for many modern communication systems such as massive MIMO [1], [2] and millimetre-wave (mmWave) [3], [4]. Massive MIMO technology supports more than one hundred antennas at the base station (BS) [5], and mmWave exploits GHz spectra to support Giga-bit-per-second (Gbit/s) data transmission [6]. However, both of them suffer from high circuit power consumption and insufferable fabrication cost due to their massive RF chains. This could be a critical problem in massive MIMO and mmWave applications requiring RF components (e.g., a high-resolution analog-digital converter (ADC) with Giga-sampling rate) with high power and high cost [7], [8].

Currently, to solve the above problems, the existing works can be divided into two potential categories. The first kind is to replace the high-resolution ADC with a low-resolution ADC (usually 1-3 bits). The second kind is to redesign the receiver with low power and low cost non-linear detector technology [9]–[14]. Non-linear receiver which reserves only phases or magnitudes of the received complex signals through phase or envelop detectors at BS can resolve

The associate editor coordinating the review of this manuscript and approving it for publication was Hayder Al-Hraishawi.

the above problems. According to our survey [15]–[17], non-linear receivership (each RF link has the 4.135 Watt) have less power consumption and cost than low-resolution ADCs (each RF link has the 9.62 Watt). This is because non-linear receivers require only one RF link, while low-resolution ADCs take advantage of low power consumption. 1-bit ADC also requires two RF links (traditional receivers require Inphase (I) and Quadrature (Q) signal components channels to modulate signals separately).

Recently, half phase-only MIMO (HPO MIMO) scheme as one of the above nonlinear MIMO systems was first proposed in [12]. This scheme is designed by using low-precision low-noise-amplifiers (LNAs), π-phase detector, and only one high-resolution ADC on each RF chain at BS side. Because cumbersome superheterodyne circuits and inphase-quadrature (IQ) demodulation have been removed, the circuit power consumption and fabrication cost of the HPO MIMO system could be much lower than that of the conventional MIMO system. Besides, in existing non-linear MIMO systems, due to the fact that the observed information is missing half dimension information, the problem of 'observation ambiguity' is encountered in channel estimation part. However, existing references show that HPO MIMO suffers less ambiguity than envelop modulation systems (also named amplitude or magnitude MIMO) [12], [18]. The ambiguity of HPO-MIMO systems has been solved [13], but the ambiguity of magnitude MIMO systems have not been solved. Therefore, it is more meaningful to study HPO MIMO system. More details about the HPO MIMO can be found in [12].

Equipping π-phase detectors on multiple antennas seems to be a promising technique for the future low power consumption communication systems [19]. Channel estimation (CE) problem in HPO MIMO system has been discussed in [13], [20]. Multiuser detection (MUD) problem in HPO MIMO system has been discussed in [12], [13], [20]. Besides, the synchronization problem in which joint time and frequency in HPO MIMO have been discussed in [13], which exploits the repeatability of a pilot preamble. Despite this growing interest in the HPO MIMO system, to explore the low-power and low-cost system from the theory aspect has received little attention to date. This paper is to fill in this gap.

The purpose of the paper is to provide an efficient method for calculating the achievable rate of the HPO MIMO system. Due to the non-linear nature of HPO MIMO, it has no closed-form solution, then we can not calculate it in the same way as traditional MIMO systems. Therefore, we seek the achievable rate of HPO MIMO from the perspective of mutual information theory. However, when we use mutual information theory, high-dimensional integration is inevitable, especially when the number of N_R, N_T is relatively large. Therefore, numerical analysis methods play a critical role here. Unfortunately, Monte Carlo (MC) method has outrageous low computational efficiency characteristics, especially in the HPO MIMO system. Therefore, it is essential to find an efficient numerical analysis method to calculate high-dimensional integrals. Based on number theory and abstract algebra, we propose a quasi-Monte Carlo (QMC) method to calculate the achievable rate of the HPO MIMO system. Antithetic variables technology as one of variance reduction techniques is used to further increase the efficiency of calculation.

The main contributions of this paper are three-fold. Firstly, the paper proposes an efficient method to calculate the uplink achievable rate for HPO MIMO. In addition, the proposed algorithm can also be used to calculate other problems with high-dimensional integrals. Secondly, this paper derives the PDF of the HPO MIMO system. Thirdly, the paper compares the performance of HPO MIMO and conventional MIMO.

The rest of this paper is organized as follows. Section II presents the details of the proposed RF chain structure and the model of HPO MIMO. Section III derives the uplink achievable rate for HPO MIMO. Section IV develops a new method for calculating achievable rate of HPO MIMO. Section V reports some simulation results which reveal the efficiency of our proposed method and performance of HPO MIMO. Section VI concludes.

Notation: $i^2 = -1$. $\mathbf{H}_{ij}$ is the (i, j)-th element of matrix $\mathbf{H}$ and $(\cdot)^H$ denotes complex-conjuate transposition. For an integer N, $[N] = 1, 2, \cdots, N$. $\Re(\cdot)$ and $\Im(\cdot)$ extract the real and imaginary parts of their complex-valued arguments, respectively. Bold lower and upper case letters stand for random vectors and matrices, respectively. $\varepsilon(\cdot)$ denote expectation. $I(\cdot)$, $h(\cdot)$ and $p(\cdot)$ denote mutual information, entropy and probability density, respectively.

II. SYSTEM MODEL

A single-cell HPO MIMO system with N_T single-antenna terminals and a BS with N_R antennas in Fig. 1 is considered [13], where each antenna is equipped with a HPO-detector (containing π-phase detector and combines with only one high revolution ADC) at the BS side.

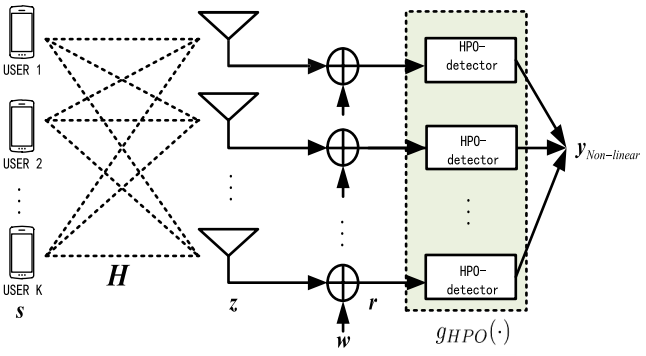

FIGURE 1. Generic HPO MIMO system model. The HPO MIMO system concludes N_T single-antenna terminals and a BS with N_R antennas. The signal received at BS after the HPO-detector $g(\cdot)$ is represented as $y_{Non-linear}$.

For the uplink, we have three assumptions: 1. all N_T users transmit independent data symbols to the BS simultaneously through the stationary memory-less flat fading channel H; 2. the sampled signal constitutes a sufficient statistic data at

the receiver; 3. in this paper, we assume H is long enough to be estimated, and changes to an independent realization come in the next block. A discrete-time baseband is considered in our model. The signal received at BS after obtaining π-phase operator $g_{HPO}(\cdot)$ is formulated as

$$\mathbf{y} = g_{HPO}\{(\mathbf{H}s + \mathbf{w})\} = g_{HPO}\{(\mathbf{z} + \mathbf{w})\} = g_{HPO}(\mathbf{r}), \quad (1)$$

where the function $g_{HPO}(\cdot)$ means the operator of obtaining π-phase of the received signal $\mathbf{y}$ as shown in equation (2). We denote $\mathbf{H}s$ by $\mathbf{z}$, and denote $\mathbf{H}s + \mathbf{w}$ by $\mathbf{r}$, and $\mathbf{s} \sim \mathcal{CN}(\mathbf{0}, \sigma_s^2\mathbf{I}_{N_T})$ is the transmitting signals by each user. It obeys the complex Gaussian distribution with $\mathbf{0}$ mean and σ_s^2 variance. $\mathbf{I}_{\mathbf{N_T}}$ represents the identity matrix with N_T dimension. In our simulation, we fix $\varepsilon(|\mathbf{s}|^2) = \mathbf{1}$. $\mathbf{w} \sim \mathcal{CN}(\mathbf{0}, \sigma_w^2\mathbf{I}_{N_R})$ is the $N_R * 1$ additive white Gaussian noise vector with $\mathbf{0}$ mean and σ_w^2 variance. $\mathbf{H}$ represents the $N_R * N_T$ channel matrix which remains constant for coherence period. Therefore, $\mathbf{r} \sim \mathcal{CN}(\mathbf{0}, \sigma_s^2\mathbf{H}\mathbf{H}^H + \sigma_w^2\mathbf{I}_{N_R})$. Due to the character of our HPO-detector, formula (1) can be extended to

$$\begin{aligned} y_{i,HPO.} &= g_{HPO.}(r_i) = \angle_\pi(r_i) \\ &= \text{atan}(r_i) \in (-\pi/2, \pi/2], \end{aligned} \quad (2)$$

where r_i is the i-th element of the vetctor $\mathbf{r}$, $i = 1, 2, \ldots, N_R$. The inverse tangent function atan$(\cdot)$ in (2) places the angle in the correct quadrant. The function $\angle_\pi(\cdot)$ is used to replace the function atan$(\cdot)$ in the following content. Due to the physical characteristics of the HPO detecter, the output signal falls within the interval of $(-\pi/2, \pi/2]$.

III. ACHIEVABLE RATE FOR HPO MIMO

We compute the achievable rates instead of capacity since the capacity of the HPO MIMO system is too cumbersome to find. The key characteristic in our HPO MIMO system is that the received signal $\mathbf{y}$ at BS side is missing half the dimensions information after HPO-detector $g_{HPO}(\cdot)$ process. Since we are considering a MIMO system, we need to consider the number of receiving antennas when calculating the achievable rate of the system. The probability of the output $\mathbf{y}$ conditioned on $\mathbf{z}$ plays a crucial role. Since the noise vector $\mathbf{w}$ is white across the receive antennas and the nonlinear function $g_{HPO}(\cdot)$ acts on each antenna separately, the conditional distribution of $\mathbf{y}$ given $\mathbf{z}$ can be factorized as

$$f(\mathbf{y}|\mathbf{z}) = \prod_{i=1}^{N_R} f(y_i|z_i), \quad (3)$$

where N_R denotes the number of receiving antennas, y_i and z_i denote the i-th elements in the real vector $\mathbf{y}$ and the complex vector $\mathbf{z}$, respectively. $\mathbf{r} \sim \mathcal{CN}(\mathbf{z}, \sigma_w^2\mathbf{I}_{\mathbf{N_R}})$ when $\mathbf{z}$ is given.

To compute the achievable rate for HPO MIMO, we first propose the following result

Theorem 1: The PDF of π-phase MIMO $y_{i,HPO} = \angle_\pi(r_i)$ is as follows

$$\begin{cases} f_{HPO}(y_i|z_i) = \begin{cases} f(y_i|z_i) + f(y_i - \pi|z_i) & y_i \in \left[0, \frac{\pi}{2}\right) \\ f(y_i|z_i) + f(y_i + \pi|z_i) & y_i \in \left[-\frac{\pi}{2}, 0\right) \end{cases} \end{cases} \quad (4)$$

where $i = 1, \ldots, N_R$,

$$f(y_i|z_i) = \frac{e^{-\rho_i}}{2\pi} + \sqrt{\frac{\rho_i}{4\pi}} e^{-\rho_i \cdot \sin^2\phi_i} \cdot \cos\phi_i \cdot \text{erfc}\left(-\sqrt{\rho_i} \cdot \cos\phi_i\right), \quad (5)$$

$\rho_i = |z_i|^2/\sigma_w^2$ and $[\Delta\phi_i = (y_i - \angle(z_i)) \text{mod} 2\pi] \in (-\pi, \pi]$. The complementary error function $\text{erfc}(x) = \frac{2}{\sqrt{\pi}} \int_x^\infty e^{-t^2} dt$.

Proof: According to [9], the PDF of 2π-phase MIMO $f(y_i|z_i)$ has the form of (5). After transforming angle, one can easily obtain the result of Theorem 1.

Since we assumed that the channel $\mathbf{H}$ is memoryless, the capacity is given by the maximum mutual information between the channel input $\mathbf{s}$ and the detector output $\mathbf{y}$. Furthermore, since $\mathbf{H}$ is known to the receiver, the channel output is the pair $(\mathbf{y}, \mathbf{H})$. The mutual information can be written as

$$I(\mathbf{s}; \mathbf{y}, H) = \varepsilon_H [I(\mathbf{s}; \mathbf{y}, \mathbf{H} = H)]. \quad (6)$$

From (1), we obtain that $\mathbf{s}$ and H are statistically independent. We can observe that $\mathbf{s}$, $\mathbf{z}$ and $\mathbf{y}$ constitute a Markov chain $\mathbf{s} \to \mathbf{z} \to \mathbf{y}$ under a given channel realization $H = \mathbf{H}$. Because $\mathbf{s}$ and $\mathbf{y}$ are conditionally independent, (6) can be upgraded to

$$I(\mathbf{s}; \mathbf{y}|H) = \varepsilon_H[I(\mathbf{z}; \mathbf{y}|\mathbf{H} = H)], \quad (7)$$

where according to the information theory, the mutual information of interest $I(\mathbf{z}; \mathbf{y}|H)$ is extended to

$$\begin{aligned} I(\mathbf{z}; \mathbf{y}|\mathbf{H}) &= h(\mathbf{y}|\mathbf{H}) - h(\mathbf{y}|\mathbf{z}, \mathbf{H}) \\ &= -\int f(\mathbf{y}|\mathbf{H}) \log(f(\mathbf{y}|\mathbf{H}))\, d\mathbf{y} \\ &\quad + \iint f(\mathbf{z},\mathbf{y}) \log(f(\mathbf{y}|\mathbf{z}))\, d\mathbf{y} d\mathbf{z}. \end{aligned} \quad (8)$$

From (7) to (8), the fact of $h(\mathbf{y}|\mathbf{z}, \mathbf{H}) = h(\mathbf{y}|\mathbf{z})$ is used. In order to calculate the mutual information of interest $I(\mathbf{z}; \mathbf{y}|\mathbf{H})$, the PDFs $f(\mathbf{y}|\mathbf{H})$ and $f(\mathbf{y}|\mathbf{z})$ are needed. Given $f(\mathbf{y}|\mathbf{z}), f(\mathbf{y}|\mathbf{H})$ can by rewritten as

$$\begin{aligned} f(\mathbf{y}|\mathbf{H}) &= \int f(\mathbf{z}|H) f(\mathbf{y}|\mathbf{z}, \mathbf{H}) d\mathbf{z} \\ &= \int f(\mathbf{z}|H) f(\mathbf{y}|\mathbf{z}) d\mathbf{z}. \end{aligned} \quad (9)$$

Combining (8) and (9), we have

$$\begin{aligned} I(\mathbf{z}; \mathbf{y}|\mathbf{H}) &= -\int f(\mathbf{y}|\mathbf{H}) \log\left\{\int f(\mathbf{z}|\mathbf{H}) f(\mathbf{y}|\mathbf{z}) d\mathbf{z}\right\} d\mathbf{y} \\ &\quad + \iint f(\mathbf{z},\mathbf{y}) \log(f(\mathbf{y}|\mathbf{z}))\, d\mathbf{y} d\mathbf{z}. \end{aligned} \quad (10)$$

where $f(y|z)$ is computed by (3) and (4).

Remark: Deriving the expression of $f(\mathbf{y}|\mathbf{H})$, $f(\mathbf{z}, \mathbf{y})$ and $f(\mathbf{z}|\mathbf{H})$ is nontrivial. Instead of trying to explore the analytical expression of them, we evaluate (8) by the idea of stochastic simulation sample mean algorithm such as Monte Carlo (MC).

MC approximate $h(\mathbf{y}|\mathbf{H}), f(\mathbf{y}|\mathbf{z},\mathbf{H})$ and $f(\mathbf{y}|\mathbf{H})$ by

$$f(\mathbf{y}|\mathbf{H}) = \backsimeq \frac{1}{M}\sum_{j=1}^{M} f(\mathbf{y_i}|\mathbf{z}_j), \tag{11}$$

$$h(\mathbf{y}|\mathbf{H}) \simeq -\frac{1}{N}\sum_{i=1}^{N} \log\left(f(\mathbf{y_i})\right), \tag{12}$$

$$h(\mathbf{y}|\mathbf{z}) \backsimeq -\frac{1}{N}\sum_{i=1}^{N} \log(f(\mathbf{y_i}|\mathbf{z}_i)), \tag{13}$$

respectively, where $\mathbf{z}_j$ as the MC samples are generated according to complex Gaussian distribution $\mathcal{CN}(0, \sigma_s^2 HH^H)$. Combining (3), (10), (11) and (13). We approximate the achievable rate for HPO MIMO as

$$I(\mathbf{z};\mathbf{y}|\mathbf{H}) \backsimeq -\frac{1}{N}\sum_{i=1}^{N} \log \frac{1}{M}\sum_{j=1}^{M}\prod_{k=1}^{N_R} f(\mathbf{y}_{i,k}|\mathbf{z}_{i,k}) + \frac{1}{N}\sum_{i=1}^{N}\sum_{k=1}^{N_R} \log f(\mathbf{y}_{i,k}|\mathbf{z}_{i,k}). \tag{14}$$

Finally, averaging (11) - (13) over many different channel response H, we can obtain the mutual information in (6).

IV. ANTITHETIC-QMC METHOD FOR CALCULATING ACHIEVABLE RATE OF HPO MIMO

In this section, we will answer why we need to use QMC sampling to calculate multi-dimensional integrals instead of traditional MC sampling methods. Also we give the details of QMC and antithetic variates method to calculate the mutual information of interest $I(\mathbf{z};\mathbf{y}|\mathbf{H})$ in HPO MIMO system.

As can be seen from formula (8), to calculate the achievable rate of the HPO MIMO system, we have to make two sampling approximations for the first term and one sampling approximation for the second term. Also, a subtraction operation is made after the above sampling approximations. As we knew, the MC sampling principle is to achieve an infinitely close to multi-dimensional integral by increasing the sampling point density, which means the more numbers of sampling points, the higher the accuracy of the multi-dimensional integral approximation. In our simulation, to obtain a stable achievable rate, the number of sampling points is at least 10,000. Therefore, our simulation requires at least 10,000*10,000 times to obtain smooth convergence. The above summarizes only under the case of the single input single output (SISO) situation. If the situation is extended to a multi-dimensional MIMO scenario, the number of simulation will increase drastically as the growth of antenna array numbers. This will make computational efficiency very low. Therefore, to increase the efficiency of multi-dimensional integration calculation becomes very necessary and essential in the HPO MIMO system.

A. MONTE CARLO

We consider MC method to calculate an integral problem, such as formula (12), (11) and (13) in Section II. We assume $f(\cdot)$ is an integral function on the unit cube $C^q = [0,1)^q$ with q-dimension. In order to calculate integral $I(f)$ as follows [21]

$$\{I(f) = \int_{C^q} f(x)dx, \tag{15}$$

we first extract random samples $P_k = \{x_k : 1 \le k \le K\}$ from C^q which obeies uniform distribution $U[0,1)^q$. Then we calculate an estimate $\hat{I}_K$ of $I(f)$ by the following formula:

$$\hat{\boldsymbol{I}}_K(f, P_k) = \frac{1}{K}\sum_{k=1}^{K} f(x_k). \tag{16}$$

The key point of the MC method is that it is necessary to extract an independent, uniformly distributed random sequence in C^q [22]. Since a certain algorithm generates such a random sequence, it also can be called the pseudo-random sequence. According to the law of large numbers, $\hat{\boldsymbol{I}}_K$ converges to $I(f)$ in probability.

Let $\sigma_f = \sqrt{Var[f(P_k)]}$, where Var denotes variance. By the central limit theorem, the integration error produced by the MC satisfies the following inequality

$$|I(f) - \hat{\boldsymbol{I}}_K(f, P_k)| \le z_{\alpha/2}\frac{\sigma_f}{\sqrt{K}} \tag{17}$$

with probability approximate $1-\alpha$, where $z_{\alpha/2}$ denotes the $\alpha/2$ quantile of Gaussian distribution $\mathcal{N}(0,1)$. Therefore, the convergency rate of MC method is $\mathcal{O}(1/\sqrt{K})$.

B. QUASI-MONTE CARLO

Different from MC, QMC methods draw on number theory and abstract algebra [23]. The basic idea of QMC methods is to replace the pseudo-random sequences in MC with low discrepancy sequences (LDS) or quasi-random sequences which are more uniform than random sequences. To measure the uniformity of a sequence, we introduce the following definition [24], [25]

Definition 1: Let $\mathbb{B}$ be a collection of all rectangles in $[0,1]^q$ with the form $\prod_{j=1}^{q}[u_j, v_j)$, $0 \le u_j \le v_j \le 1$ and let $m(B)$ be the volume of B. The discrepancy D_K of the piont set $\{x_1, x_2, \ldots, x_K\}$ relative to $\mathbb{B}$ is defined as

$$D_K = \sup_{B\in\mathbb{B}} \left| \frac{\#\{x_i \in B\}}{K} - m(B) \right|, \tag{18}$$

where $\#\{x_i \in B\}$ denotes the number of x_i contained in B.

According to the law of iterated logarithms, if a sequence is random, the expectation of the discrepancy of the sequence is bounded by $\log\log K/\sqrt{K}$. In contrast, the discrepancy of many low discrepancy sequences such as Halton sequence is bounded by constant times $(\log K)^q/K$.

1) HALTON' LDS

Any non-negative integer k can be constituted as the following form based on the prime number b:

$$k = d_j b^j + d_{j-1}b^{j-1} + \ldots + d_1 b + d_0, \tag{19}$$

where $d_i \in \{0, 1, \ldots, b-1\}, i = 0, 1, \ldots, j$, $b^j \le k < b^{j+1}$.

We define the radical inverse function $\varphi_b(k)$ based on b as follows:

$$\varphi_b(k) = \frac{d_0}{b^1} + \frac{d_1}{b^2} + \ldots + \frac{d_j}{b^{j+1}}, \tag{20}$$

it's easy to find for any integer $k \geqslant 0$, $\varphi_b(k) \in [0, 1]$.

To obtain Halton' LDS $\{x_1, \ldots, x_m\}$ of length m with d-dimensional, we take d different prime numbers $b_1, \ldots, b_d$ as base. Then let $x_k = \left[\varphi_{b_1}(k-1), \ldots, \varphi_{b_d}(k-1)\right]^T$, where $k = 1, \ldots, m$. In fact, it is no need to generate the Halton sequence starting from $k = 0$. That is to say, for d non-negative integers $n_1, \ldots, n_d$, the above sequence can be taken as $x_k = \left[\varphi_{b_1}(n_1 + k - 1), \ldots, \varphi_{b_d}(n_d + k - 1)\right]^T$. We can generate Halton' LDS by the following algorithm

Algorithm 1 An Algorithm for Generating Halton' LDS

Input: base $b_1, b_2, \ldots, b_d, k$
for $i = 1$ *to* d **do**
  $b_{ki} = 0$;
  $j = 0$;
  for $k \neq 0$ **do**
    $b_{ki} = b_{ki} + mod(k, b_i)/b_i^{j+1}$;
    $k = floor(k/b_j)$;
    $j = j + 1$ end;
  Output b_{ki};

Niederreiter [26] states that the discrepancy of Halton sequence satisfies that

$$D_K \leq c_q \frac{(\log K)^q}{K} + \mathcal{O}\left(\frac{(\log K)^{q-1}}{K}\right), \tag{21}$$

where c_q is a constant which only depends on dimension q. (18) implies that the Halton sequence is significantly more uniform than a random sequence.

2) ERROR BOUND OF QMC

The integration error produced by QMC satisfies the following Koksma-Halwka inequality.

$$|I(f) - \hat{\boldsymbol{I}}_K(f, P_k)| \leqslant V(f) D_K, \tag{22}$$

where D_K is the discrepancy of the sequence P_K. The variation $V(f)$ in (22) of $f(x)$ in the sense of Hardy and Krause is defined as:

$$V(f) = \sum_{k=1}^{s} \sum_{1 \leq i_1 < i_2 < \ldots < i_k \leq s} V^{(k)}(f; i_1, \ldots, i_k). \tag{23}$$

If $f(x_1, \ldots, x_s)$ is sufficiently differentiable, for all positive $k \leq s$ and k integers $1 \leq i_1 < i_2 < \ldots < i_k \leq s$, define the quantity as follows:

$$V^{(k)}(f; i_1, \ldots, i_k) = \int_{l^k} \left| \frac{\partial^k f}{\partial t_{i_1} \ldots \partial t_{i_k}} \right|_{t_j = 1, j \neq i_l, \ldots i_k} dt_{i_1} \ldots dt_{i_k}. \tag{24}$$

(23) and (24) imply that once $f(\cdot)$ is given, $V(f)$ would be a constant. Therefore, the integration error produced by QMC only depends on D_K. From (18), the convergency rate of QMC method based on Halton sequence is $\mathcal{O}\left(\frac{(\log K)^{q-1}}{K}\right)$. Since $(\log K)^{q-1}$ can be absorbed into any power of K, the convergency rate of QMC method can be thought as near $\mathcal{O}(1/K)$. Therefore, QMC methods accelerate convergence from $\mathcal{O}(1/\sqrt{K})$ of MC methods to nearly $\mathcal{O}(1/K)$.

Statisticians focus on how to construct the best low discrepancy (quasi-random) point sets [27]–[30]. At the same time, variance reduction techniques [31], [32] are widely studied from another side for improving the efficiency of such sampling methods. In our work, we combine the flexibility of variance reduction techniques with the characteristic of effectiveness and fast convergence of low discrepancy sequences. We not only use the Halton sequences as our low discrepancy point sets, but also combine antithetic variates technique as the variance reduction techniques, and the detail can be found in the following part.

C. ANTITHETIC VARIATES TECHNIQUE

Antithetic variates is one of variance reduction techniques [33] for MC sample [34], [35]. It attempts to reduce variance by introducing negative dependence between pairs of sampling points [36]. If U is uniformly distributed over $[0, 1]$, then $1 - U$ obeys uniform distribution, too. According to this principle, if we generate $U_1, \ldots, U_n$ as the first path, then we still can generate $1 - U_1, \ldots, 1 - U_n$ as the second path without changing the law of this simulation process. Antithetic variates technique reduce the variance based on the following fact

$$\begin{aligned} \mathrm{Cov}[U, (1-U)] &= \mathrm{E}[U(1-U)] - \mathrm{E}[U]\mathrm{E}[1-U] \\ &= \mathrm{E}[U - U^2] - \mathrm{E}[U](1 - \mathrm{E}[U]) \\ &= \mathrm{E}^2[U] - \mathrm{E}[U^2] \\ &= -\mathrm{D}[U] < 0, \end{aligned} \tag{25}$$

where $\mathrm{Cov}[\cdot, \cdot]$ denotes the covariance. In particular, for Gaussian distributions commonly used in telecommunications, antithetic variates can be implemented by pairing the sequences $Y_1, Y_2, \ldots$ of independently and identically distributed (i.i.d.) $\mathcal{CN}(0, 1)$ variables. The key characteristics of the antithetic variates technologies is that for each i, Y_i and $\tilde{Y}_i$ have the same distribution, and all the pairs $(Y_1, \tilde{Y}_1), (Y_2, \tilde{Y}_2), \ldots, (Y_n, \tilde{Y}_n)$ are i.i.d.

The antithetic variates estimator $\hat{Y}_{AV}$ is the average of all $2n$ observations from the common distribution of Y_i and $\tilde{Y}_i$,

$$\hat{Y}_{AV} = \frac{1}{2n}\left(\sum_{i=1}^{n} Y_i + \sum_{i=1}^{n} \tilde{Y}_i\right) = \frac{1}{n}\sum_{i=1}^{n}\left(\frac{Y_i + \tilde{Y}_i}{2}\right), \tag{26}$$

the variance can be written as

$$\begin{aligned} \mathrm{Var}[Y_i + \tilde{Y}_i] &= \mathrm{Var}[Y_i] + \mathrm{Var}[Y_i] + 2\mathrm{Cov}[Y_i, \tilde{Y}_i] \\ &= 2\mathrm{Var}[Y_i] + 2\mathrm{Cov}[Y_i, \tilde{Y}_i] \\ &< 2\mathrm{Var}[Y_i], \end{aligned} \tag{27}$$

because Y_i and $\tilde{Y}_i$ have the same distribution, the variance of Y_i and $\tilde{Y}_i$ are the same. The condition for antithetic sampling to reduce variance becomes

$$\mathrm{Cov}[Y_i, \tilde{Y}_i] < 0, \tag{28}$$

therefore,

$$\mathrm{Var}[\hat{Y}_{AV}] < \mathrm{Var}\left[\frac{1}{2n}\sum_{i=1}^{2n} Y_i\right]. \tag{29}$$

(26) implies that the efficiency of the MC method is increased after introducing an antithetic variate. This technique can also be applied in the QMC method.

D. ANTITHETIC-QMC METHOD

We combine antithetic variates technique and QMC method and propose the Antithetic-QMC method to calculate uplink achievable rate for HPO MIMO systems. We develop Antithetic-QMC algorithm as follows:

Algorithm 2 Antithetic-QMC Algorithm for Calculating the Uplink Achievable Rate for HPO MIMO System

Input: $N_T, N_R, N_1, N_2, H, W, \phi_k, \rho_k, (k = 1, \ldots, N_R)$;
$S_{um11} = 0, S_{um12} = 0, S_{um2} = 0, S_{um31} = 0, S_{um32} = 0$
for $i = 1$ *to* N_2 **do**
  Draw Halton sequence $y_{i,2}$ by Algorithm 1;
  for $j = 1$ *to* N_1 **do**
    Draw Halton sequence $y_{i,j,1}$ by Algorithm 1;
    Compute $f(y_{i,j,1}|z_{i,j})$ and $f(y_{i,j,2}|z_{i,j})$ by (3);
    $S_{um11} = S_{um11} + f(y_{i,j,1}|z_{i,j})$;
    $S_{um12} = S_{um12} + f(y_{i,j,2}|z_{i,j})$;
    until the last simulation;
  $S_{um2} = S_{um2} + \log\frac{S_{um11}+S_{um12}}{2N_1}$;
  $S_{um31} = S_{um31} + \log f(y_{i1}|z_i)$;
  $S_{um32} = S_{um32} + \log f(y_{i2}|z_i)$;
  until the last simulation;
Compute $h(y|H)$ by $-\frac{S_{um2}}{N_2}$;
Compute $h(y|z)$ by $-\frac{S_{um31}+S_{um32}}{2N_2}$;
Compute achievable rate by (8).

V. NUMERICAL RESULTS

In this section, we present some numerical experiments to confirm the analysis in the previous parts. To verify the correctness of the PDF of HPO MIMO system which we derived, we first compare the histogram of HPO MIMO distribution and the PDF of HPO MIMO. In the following numerical simulations, the input s of transmitter follows by Complex Gaussian distribution $s \sim \mathcal{CN}(0, \sigma_s^2 I_{N_T})$. The channel matrix entries H are modeled as i.i.d. zero-mean unit-variance circularly symmetric Gaussian random variables. Where we assume $\sigma_s^2 = 1$ and $\sigma_h^2 = 1$. The received vector z is perturbed by a zero-mean circularly symmetric Gaussian noise vector w, with autocorrelation function $E[\mathbf{w_k}\mathbf{w}_l] = \sigma_w^2 \mathbf{I}_{N_R}\delta(k-l)$, where k and l are symbol instants, and we let $\sigma_w^2 = \frac{N_T\sigma_s^2}{\mathrm{SNR}}$. We assume all users have the same level of SNR in our experiments.

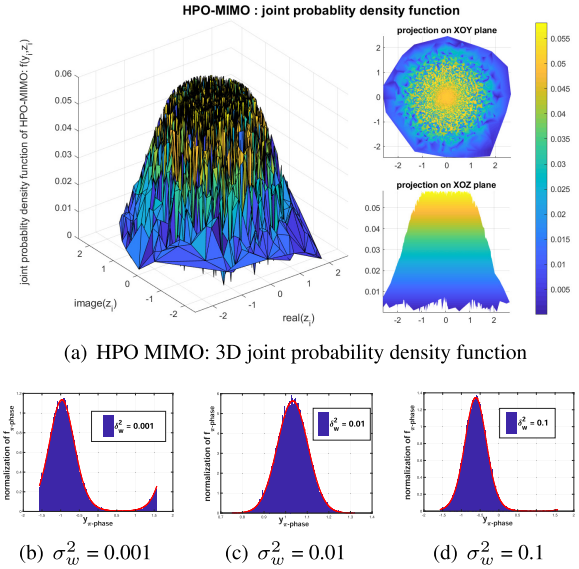

(a) HPO MIMO: 3D joint probability density function

(b) $\sigma_w^2 = 0.001$ (c) $\sigma_w^2 = 0.01$ (d) $\sigma_w^2 = 0.1$

FIGURE 2. 3D joint probability density function of HPO MIMO and corresponding 2D histogram of probability density function $y_{\pi-phase}$. (a) shows the 3D joint probability density function of HPO MIMO $f(y_i, z_i)$. (b)(c)(d) show the 2D histogram of probability density function $y_{\pi-phase}$ under the different variance of Gaussian noise $\sigma_w^2 = 0.001$, $\sigma_w^2 = 0.01$ and $\sigma_w^2 = 0.1$, respectively.

Fig. 2 (a) shows our derived 3D joint PDF $f(y_i, z_i)$ of HPO MIMO, imaginary part and real part of z_i are used to illustrate $f(y_i, z_i)$. In order to describe our derived PDF $f(y_i, z_i)$ of HPO MIMO more clearly, we plot the corresponding 2D histogram of PDF $y_{\pi-phase}$ under the different variance σ_w^2 of Gaussian noise in Fig. 2 (b), (c) and (d), respectively. We randomly generate the HPO MIMO distributions y_{HPO} according to the phase-obtaining operation $g_\pi\{(Hs + w)\}$, and draw their normalized histograms as shown in the blue columns. At the same time, we plot the HPO MIMO PDF $f_{HPO}(y_i|z_i)$ as shown in the red line which we derived from (3). It can be seen that these blue columns and the red line are closely matched under the different noise σ_w^2. Those results confirm the correctness of our derived PDF $f_{HPO}(y_i|z_i)$ in (3).

To test the uniformity of Halton' LDS, we implement algorithm 1 and compare distributions of $N_1 = 4$ (Fig. 3) and $N_2 = 16$ (Fig. 4) points on a unit square $n = 2$ given by two different sampling techniques: MC and Halton' LDS. This provides a qualitative picture of the uniformity properties of these sampling techniques. In the first case, the unit square is divided into 4 and 4^2 squares of measure $1/4$ and $1/4^2$, respectively. In the second case, the unit square is divided into 16 and 16^2 squares of measure $1/16$ and $1/16^2$, respectively. Fig. 3/ Fig. 4 (c), (d) show 2-dimensional distributions of Halton' points, and each of the 4 small squares contains exactly one Halton' point. Random sampling MC (Fig. 3/ Fig. 4 (a), (b)) do not possess either of these properties.

Fig. 5 shows distributions of 64 points in two dimensions. From Fig. 5 (c), it is clear that each of the 64^2 subsquares

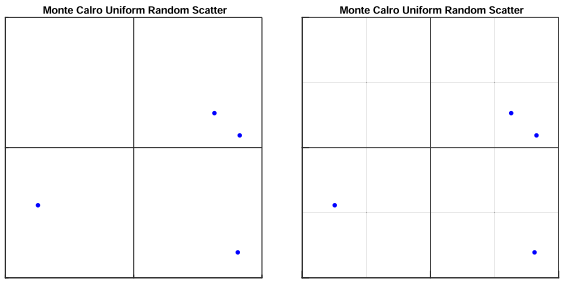

(a) Monte Carlo 4 points (b) Monte Carlo 4 points

(c) Halton' LDS 4 points (d) Halton' LDS 4 points

FIGURE 3. Distributions of 4 points in two dimensions. The unit square is divided into 4 parts as shown on the left and 16 parts as shown on the right.

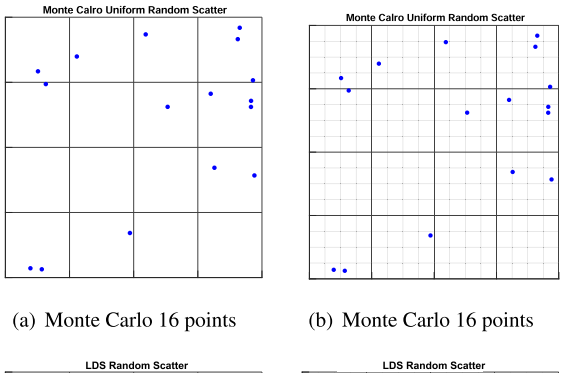

(a) Monte Carlo 16 points (b) Monte Carlo 16 points

(c) Halton' LDS 16 points (d) Halton' LDS 16 points

FIGURE 4. Distributions of 16 points from two dimensions. The unit square is divided into 16 parts, as shown on the left and 256 parts, as shown on the right.

contains exactly 1 Halton' point (Fig. 5 (d)). And this phenomenon is existing in all types of MC (Fig. 5 (a)) samplings: clustering and empty subsquares are clearly visible from these plots (Fig. 5 (b)). From Fig. 3 to Fig. 5, in summary it

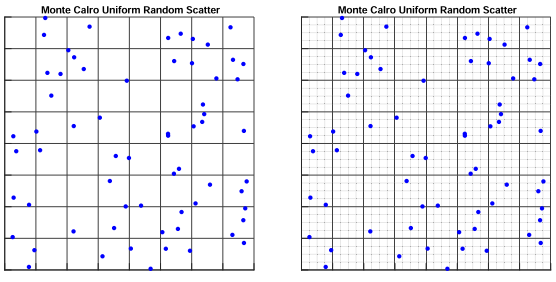

(a) Monte Carlo 64 points (b) Monte Carlo 64 points

(c) Halton' LDS 64 points (d) Halton' LDS 64 points

FIGURE 5. Distributions of 64 points in two dimensions. The unit square is divided into 64 parts, as shown on the left and 4096 parts, as shown on the right.

	Monte Carlo (MC)	Halton' LDS
The sequence method	Pseudorandom sequence	Low-discrepancy sequence (Halton sequence)
The distribution of the sampling points	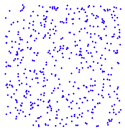	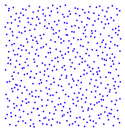

FIGURE 6. Monte-Carlo (MC) v.s. the Halton' LDS under same simulation duration. In our simulation, the number of simulation is 10*10000*10000.

would appear that Halton' LDS sampling gives a better way of arranging N points in n dimensions than MC method.

Furthermore, we extracted 2000 points from the two-dimensional unit square using the MC method and the Halton' LDS, respectively. From Fig. 6, we can see that the points using the Halton' LDS method are more uniformly, whereas the points using the MC sampling method are denser in some places and sparse in others. Fig. 6 shows that Halton' LDS has smaller standard error than MC.

To test the efficiency of the Antithetic-QMC method, we implement algorithm 2 and compare Antithetic-QMC with MC and QMC. MC and QMC for computing achievable rate of HPO MIMO can be implemented by modifying algorithm 2. The MC estimate $\hat{\boldsymbol{I}}$ converges to the true value of $\boldsymbol{I}$ as sample points N approaches to infinity by the law of large numbers. Therefore we calculate the accurate value of $\boldsymbol{I}$ by MC method. A comparison of methods

requires a figure of merit. For sampling-based methods, standard error is an appropriate figure of merit [37]. As our figure of merit, we take $\log 2$ of standard error δ, where $\delta = \frac{\sqrt{\sum_{i=1}^{N}(f(x_i)-I(N))}}{\sqrt{N}}$. The smaller $\log 2\delta$, the higher efficiency of calculating.

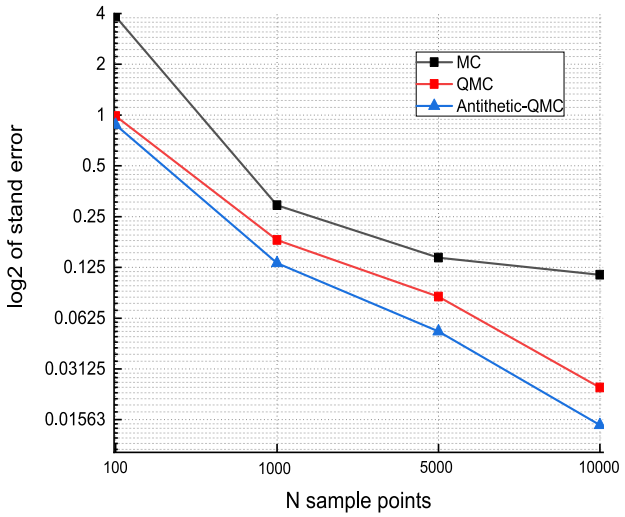

FIGURE 7. Comparison of the convergency rate among MC, QMC and Antithetic-QMC for calculating the achievable rate for HPO MIMO systems.

Fig. 7 compares the $\log 2$ of standard error among MC, QMC and Antithetic-QMC for calculating the achievable rate for HPO MIMO systems with simulation trials $N = 100, 1000, 5000$ and 10000, respectively. The reason for the choice of 10000 as the limit is that in the variance reduction technique, the standard error $\delta = 0.02$ marks the result of the sampling method close to the multi-dimensional integral result. Fig. 7 shows that QMC converges fast, and the standard error is significantly smaller than MC. Antithetic-QMC further increases the convergency rate compared to QMC.

The performance of Antithetic-QMC is slightly better than QMC at a high number of samples. However, these two methods have much better performance than traditional MC methods, especially at higher sampling numbers. This is precise because both of these QMC methods use a more uniform LDS sequence instead of a random sequence in calculating the multi-dimensional integration in the HPO MIMO system. We can conclude that Antithetic-QMC is superior to QMC and MC in calculating uplink achievable rate for HPO MIMO system.

With the proposed method we compare the achievable rate between the HPO MIMO and the conventional MIMO under the SISO and MIMO scenario. Fig. 8 reports the main outcomes.

Fig. 8 presents two key phenomena. Firstly, with the increase of the signal-to-noise ratio (SNR) from -10dB to 30dB, achievable rate keeps increasing. Secondly, HPO MIMO always achieves more than half the performance of its corresponding conventional MIMO. Although the

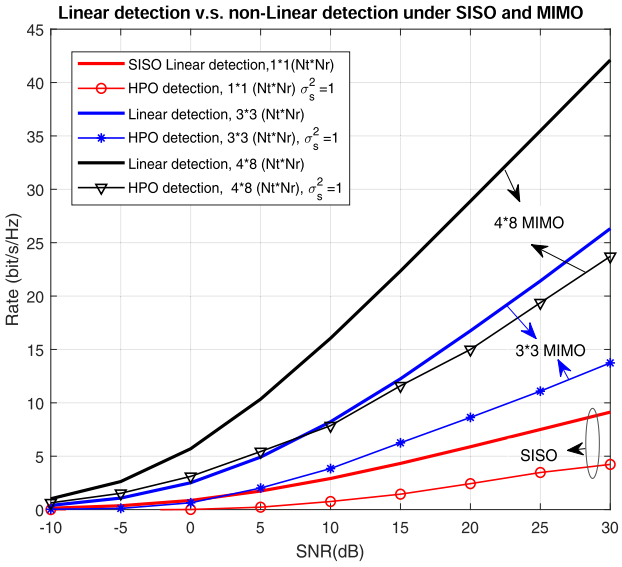

FIGURE 8. Linear detection v.s. non-Linear (HPO) detection under different scenarios, including 8*4 MIMO, 3*3 MIMO and SISO. Rayleigh fading channel used in this simulation. The solid lines stand for linear MIMO detection, and line with triangle, star and circle stand for half phase only (HPO-) MIMO detection under 8*4 MIMO, 3*3 MIMO and SISO, respectively.

performance of HPO MIMO is inferior to that of conventional MIMO, we do prefer π-phase detection. This is because cumbersome demodulation is removed, and no analog combination of IQ signals is required as conventional MIMO, its circuit power and costs are much lower than its corresponding MIMO [11]. This result indirectly indicates that HPO MIMO can achieve the rates of conventional MIMO by increasing the number of antennas at the receiver. The results show that the HPO MIMO system can obtain $50\% - 67\%$ of the capacity of traditional MIMO with only little power consumption compare to the conventional MIMO system. This conclusion proves that HPO MIMO is a promising technology in future low-power communication scenarios.

VI. CONCLUSION AND FUTURE

We derive a semi-analytical expression of the achievable rate for HPO MIMO system, in which high-dimensional integrals are approximated numerically by quasi-Monte Carlo and antithetic variates technique. Our proposed method speeds up the computational efficiency of the achievable rate for the HPO MIMO system compared to Monte Carlo and quasi-Monte Carlo methods. The high accuracy can be obtained by increasing sampling points numbers. Therefore, our method can be used as a benchmark for testing efficiency of other analytical approximation or numerical methods to calculate the achievable rate.

With our proposed method, we provide a comparison on the achievable rates of HPO MIMO and conventional MIMO systems. Our comparison results show that although the performance of HPO MIMO is not as good as its corresponding linear detection (which can be achieved more than half),

these low-power consumption techniques unexpectedly utilize additional receive antennas to achieve higher spatial multiplexing gain. This result seems promising since it could save more power and cost to use more HPO-receiver RF chains than the conventional ones.

REFERENCES

[1] A. Mishra and T. Alexander, "Radio communications: Components, systems, and networks," *IEEE Commun. Mag.*, vol. 53, no. 3, p. 189, Mar. 2015.

[2] X. Ge, Y. Sun, H. Gharavi, and J. Thompson, "Joint optimization of computation and communication power in multi-user massive MIMO systems," *IEEE Trans. Wireless Commun.*, vol. 17, no. 6, pp. 4051–4063, Jun. 2018.

[3] W. Wang, S. He, Y. Wu, H. Wang, Y. Huang, and L. Yang, "Performance evaluation and analysis of millimeter wave communication system," *IEEE Syst. J.*, vol. 13, no. 1, pp. 159–170, Mar. 2019.

[4] X. Wang, L. Kong, F. Kong, F. Qiu, M. Xia, S. Arnon, and G. Chen, "Millimeter wave communication: A comprehensive survey," *IEEE Commun. Surveys Tuts.*, vol. 20, no. 3, pp. 1616–1653, 3rd Quart., 2018.

[5] J. Zhang, L. Dai, X. Li, Y. Liu, and L. Hanzo, "On low-resolution ADCs in practical 5G millimeter-wave massive MIMO systems," *IEEE Commun. Mag.*, vol. 56, no. 7, pp. 205–211, Jul. 2018.

[6] P. Kumari, K. U. Mazher, A. Mezghani, and R. W. Heath, "Low resolution sampling for joint millimeter-wave MIMO communication-radar," in *Proc. IEEE Stat. Signal Process. Workshop (SSP)*, Jun. 2018, pp. 193–197.

[7] X. Ge, J. Yang, H. Gharavi, and Y. Sun, "Energy efficiency challenges of 5G small cell networks," *IEEE Commun. Mag.*, vol. 55, no. 5, pp. 184–191, May 2017.

[8] J. Hoydis, S. ten Brink, and M. Debbah, "Massive MIMO: How many antennas do we need?" in *Proc. 49th Annu. Allerton Conf. Commun., Control, Comput. (Allerton)*, Sep. 2011, pp. 545–550.

[9] G. K. Psaltopoulos, F. Troesch, and A. Wittneben, "On achievable rates of MIMO systems with nonlinear receivers," in *Proc. IEEE Int. Symp. Inf. Theory*, Jun. 2007, pp. 1071–1075.

[10] G. K. Psaltopoulos and A. Wittneben, "Achievable rates of nonlinear MIMO systems with noisy channel state information," in *Proc. IEEE Int. Symp. Inf. Theory*, Jul. 2008, pp. 2659–2662.

[11] S. Wang, L. Zhang, Y. Li, J. Wang, and E. Oki, "Multiuser MIMO communication under quantized phase-only measurements," *IEEE Trans. Commun.*, vol. 64, no. 3, pp. 1083–1099, Mar. 2016.

[12] S. Wang, M. He, Q. Guo, and L. Zhang, "Nonlinear MIMO communications under pi-periodic phase measurements," in *Proc. IEEE Global Commun. Conf. (GLOBECOM)*, Dec. 2018, pp. 1–6.

[13] S. Wang, M. He, and X. Jiang, "Joint time and frequency synchronization in halved phase-only MIMO," *IEEE Trans. Veh. Technol.*, vol. 68, no. 8, pp. 8201–8205, Aug. 2019.

[14] C. Wang, M. Liang, and Y. Chai, "Adaptive neural network control of a class of fractional order uncertain nonlinear MIMO systems with input constraints," *Complexity*, vol. 2019, Nov. 2019, Art. no. 1410278.

[15] W. Kester. (2009). *ADC Architectures II: Successive Approximation ADCs*. [Online]. Available: http://www.analog.com/media/en/training-seminars/tutorials/MT-021.pdf

[16] Analog Company. *Website*. [Online]. Available: http://www.analog.com/cn/index.html

[17] TI Company. *Website*. [Online]. Available: http://www.analog.com/cn/index.html

[18] S. Wang, L. Zhang, and X. Jing, "Phase retrieval motivated nonlinear MIMO communication with magnitude measurements," *IEEE Trans. Wireless Commun.*, vol. 16, no. 8, pp. 5452–5466, Aug. 2017.

[19] I. Chihi and M. Benrejeb, "Online fault detection approach of unpredictable inputs: Application to handwriting system," *Complexity*, vol. 2018, Dec. 2018, Art. no. 9789060.

[20] S. Wang, Y. Li, and J. Wang, "Multiuser detection in massive MIMO with quantized phase-only measurements," in *Proc. IEEE Int. Conf. Commun. (ICC)*, Jun. 2015, pp. 4576–4581.

[21] N. Metropolis and S. Ulam, "The monte carlo method," *J. Amer. Stat. Assoc.*, vol. 44, no. 247, pp. 335–341, 1949.

[22] I. Sobol, *A Primer for Monte Carlo Method*. Boca Raton, FL, USA: CRC Press, Apr. 2018.

[23] P. A. Acworth, M. Broadie, and P. Glasserman, "A comparison of some Monte Carlo and quasi Monte Carlo techniques for option pricing," in *Monte Carlo Quasi-Monte Carlo Methods*, H. Niederreiter, P. Hellekalek, G. Larcher, and P. Zinterhof, eds. New York, NY, USA: Springer, 1998, pp. 1–18.

[24] A. B. Owen, *Multidimensional Variation for Quasi-Monte Carlo*. Singapore: World Scientific, Jan. 2014, pp. 49–74.

[25] J. Dick, F. Y. Kuo, and I. H. Sloan, "High-dimensional integration: The quasi-Monte Carlo way," *Acta Numerica*, vol. 22, pp. 133–288, May 2013.

[26] H. Niederreiter, *Random Number Generation and Quasi-Monte Carlo Methods*. Philadelphia, PA, USA: Society for Industrial and Applied Mathematics, Jul. 1992.

[27] J. H. Halton, "On the efficiency of certain quasi-random sequences of points in evaluating multi-dimensional integrals," *Numerische Math.*, vol. 2, no. 1, pp. 84–90, Dec. 1960.

[28] B. Montrucchio and R. Ferrero, "Toner savings based on quasi-random sequences and a perceptual study for green printing," *IEEE Trans. Image Process.*, vol. 25, no. 6, pp. 2635–2646, Jun. 2016.

[29] H. Liu and T. Y. Chen, "Randomized quasi-random testing," *IEEE Trans. Comput.*, vol. 65, no. 6, pp. 1896–1909, Jun. 2016.

[30] T. Speidel, J. Paul, S. Wundrak, and V. Rasche, "Quasi-random single-point imaging using low-discrepancy k -Space sampling," *IEEE Trans. Med. Imag.*, vol. 37, no. 2, pp. 473–479, Feb. 2018.

[31] X. Wang, "Variance reduction techniques and quasi-monte carlo methods," *J. Comput. Appl. Math.*, vol. 132, no. 2, pp. 309–318, 2001.

[32] Z. Cheng and Z. Lu, "A novel efficient feature dimensionality reduction method and its application in engineering," *Complexity*, vol. 2018, Oct. 2018, Art. no. 2879640.

[33] S. Biruk, P. Jaskowski, and A. Czarnigowska, "Assessing the efficiency of variance reduction methods in the construction project network simulation," *IOP Conf. Ser., Mater. Sci. Eng.*, vol. 603, no. 3, 2019, Art. no. 032094.

[34] G. S. Fishman, "Antithetic variates and quasirandom points as variance reduction techniques," in *Proc. 15th Conf. Winter Simulation WSC*, vol. 2, 1983, pp. 557–560.

[35] R. C. H. Cheng, "The use of antithetic variates in computer simulations," *J. Oper. Res. Soc.*, vol. 33, no. 3, pp. 229–237, Mar. 1982.

[36] L. Wu and M. Shahidehpour, "A hybrid model for day-ahead price forecasting," *IEEE Trans. Power Syst.*, vol. 25, no. 3, pp. 1519–1530, Aug. 2010.

[37] W. J. Morokoff and R. E. Caflisch, "Quasi-monte carlo integration," *J. Comput. Phys.*, vol. 122, no. 2, pp. 218–230, Dec. 1995.

YI GONG (Student Member, IEEE) received the B.S. degree in information and engineering from the Xi'an University of Posts and Telecommunications (XUPT), Xi'an, Shaanxi, China, in 2013, and the M.S. degree from the School of Information and Telecommunication Engineering, Beijing University of Posts and Telecommunications (BUPT), Beijing, China, in 2016. She is currently pursuing the two Ph.D. degrees with BUPT and the Global Big Data Technologies Centre, University of Technology (UTS), Sydney, NSW, Australia. Her research interests include channel modeling in vehicle networks, massive MIMO, low-power communications, and non-linear MIMO.

LIN ZHANG (Member, IEEE) received the B.S. and Ph.D. degrees from the Beijing University of Posts and Telecommunications (BUPT), Beijing, China, in 1996 and 2001, respectively. He was a Postdoctoral Researcher with the Information and Communications University, Daejeon, South Korea, from December 2000 to December 2002. He went to Singapore and held a research fellow position with Nanyang Technological University, Singapore, from January 2003 to June 2004. He joined BUPT, in 2004, as a Lecturer, then an Associate Professor, in 2005, and a Professor, in 2011. He is currently the Dean of the School of Information and Communication Engineering, BUPT. He has served the university as the Director of Faculty Development Center and the Deputy Dean of Graduate School. He has authored more than 120 articles in referenced journals and international conferences. His research interests include mobile cloud computing and the Internet of Things.

KEPING YU (Member, IEEE) received the M.E. and Ph.D. degrees from the Graduate School of Global Information and Telecommunication Studies, Waseda University, Tokyo, Japan, in 2012 and 2016, respectively.

He was a Research Associate with the Global Information and Telecommunication Institute, Waseda University, from 2015 to 2019, where he is currently a Junior Researcher. He has hosted and participated in a lot of research projects, including the Ministry of Internal Affairs and Communication (MIC) of Japan, the Ministry of Economy, Trade and Industry (METI) of Japan, the Japan Society for the Promotion of Science (JSPS), the Advanced Telecommunications Research Institute International (ATR) of Japan, Keihin Electric Railway Corporation of Japan, and Maspro Denkoh Corporation of Japan. He is also the Leader and a coauthor of the comprehensive book *Design and Implementation of Information-Centric Networking* (Cambridge University Press, 2020). He was involved in many standardization activities organized by ITU-T and ICNRG of IRTF and contributed to the ITU-T Standards ITU-T Y.3071: Data Aware Networking (Information Centric Networking) Requirements and Capabilities and Y.3033-Data Aware Networking-Scenarios and Use Cases. His research interests include smart grids, information-centric networking, the Internet of Things, blockchain, and information security. He has had experience with editorial and conference organizations. Moreover, he has served as a TPC Member for the ITU Kaleidoscope 2020, the IEEE VTC2020-Spring, the IEEE CCNC 2020, the IEEE WCNC 2020, the IEEE VTC2019-Spring, ITU Kaleidoscope 2019, the IEEE HotICN 2019, the IEEE ICCC 2019, the IEEE WPMC 2019, EEI 2019, and ICITVE 2019. He has served as the General Co-Chair and a publication Co-Chair for the IEEE VTC2020-Spring EBTSRA Workshop, a TPC Co-Chair for SCML2020, and the Session Chair for ITU Kaleidoscope 2016. He is also an Editor of the IEEE Open Journal of Vehicular Technology.

RENPING LIU (Senior Member, IEEE) received the B.E. and M.E. degrees from the Beijing University of Posts and Telecommunications, China, and the Ph.D. degree from the University of Newcastle, Australia.

He is currently a Professor and the Head of the Discipline of Network and Cybersecurity, University of Technology Sydney. He is also the Co-Founder and a CTO of Ultimo Digital Technologies Pty Ltd., developing the Internet of Things (IoT) and blockchain. Prior to that, he was a Principal Scientist and the Research Leader with CSIRO, where he led wireless networking research activities. He specializes in system design and modeling and has delivered networking solutions to a number of government agencies and industry customers. He has over 150 research publications and has supervised over 30 Ph.D. students. His research interests include wireless networking, cybersecurity, and blockchain.

Dr. Liu was a recipient of the Australian Engineering Innovation Award and the CSIRO Chairman Medal. He was the Founding Chair of the IEEE NSW VTS Chapter. He has served as the Technical Program Committee Chair and the Organizing Committee Chair in a number of IEEE conferences.